Journal of the Physical Society of Japan
Vol. 58, No. 8, August, 1989, pp. 3001-3012

Time-Dependent Spectrum of a Two-Level System Coupled to a Heat Bath Driven by Pulsed Laser

Yoshitaka TANIMURA* and Ryogo KUBO

Department of Physics, Faculty of Science and Technology, Keio University, Kohoku-ku, Yokohama 223

(Received March 15, 1989)

A two-level system diagonally coupled to a heat bath consisting of harmonic oscillators with a proper frequency spectrum producing a Markoffian random perturbation is considered. Assuming relatively weak or fast modulation conditions, we calculate spectra from the system driven by a continuous wave and a pulsed laser of arbitrary strength by applying the physical spectrum proposed by Eberly and Wódkiewicz. The results give the coherent and the incoherent spectra; clarification of how dynamical evolution of these components is influenced by the change of physical parameters is obtained.

§1. Introduction

Due to the progress in pulsed laser technique, there has been a growing interest in time-dependent resonance scattering.[1-4] Investigation of this sort of problem has always been regarded as a means of studying relaxation processes. This technique also allows us to look into the effects of perturbation from a bath on the coherence property of a scattering process. It is well known that an emission spectrum from a system interacting with a bath driven by a laser consists of coherent and incoherent components.[5-10] The coherent component, such as the Rayleigh or the Raman scattering, conserves the quantum phase coherence, whereas the coherence is interrupted in an incoherent process, which is usually called the fluorescence or the luminescence, by the perturbation from the bath. In the study of the *continuous wave* (CW) response spectrum, separation of these components is relatively simple for a commonly assumed white-noise bath, since the coherence is then completely destructed by the random perturbation. But, for a colored-noise bath, the separation of these components is difficult, since in this case there appears a mixture of the coherent and incoherent processes called the broadened Raman or the broadened Rayleigh scattering.[11-15] An analysis of the time-dependent spectrum gives us a deeper understanding of the problem and allows us more detailed considerations.

The present paper reports the CW and time-dependent emission spectrum from a two-level system which is diagonally interacting with a bath and is driven by a CW and a pulsed laser of arbitrary strengths. The spectrum we calculate here is the *physical spectrum* proposed by Eberly *et al.*[1,2] This problem has been treated by Czub and Kryszewski for a three-level system diagonally interacting with the white-noise bath.[16] We extend their treatment to the colored-noise bath by making use of our previous theory which was developed with regard to the stochastic Gaussian-Markoffian approach.[17-19] Here, we simplify the model by assuming that the system-bath interaction is relatively weak in comparison to the inverse correlation time of the interaction. This is the same as supposing a relatively fast modulation rate for the bath. This simplified model is equivalent to the stochastic two-state jump model where the random variable of the bath takes only two values.

This paper is organized in the following way. In the next section we formulate, using our previous formalism, the time evolution of a two-level system coupled to a bath and driven by a CW and pulsed laser. In §3 we pre-

* Present address: Beckman Institute, University of Illinois, 405 N. Mathews, Urbana, IL 61801, U.S.A.

sent the physical spectrum from this two-level system. In §4 we calculate these spectra for the diagonal modulation model. In this study we show that the effect of modulation acts on the Liouvillian of the system as the additional damping and frequency shift. In §5 we discuss the very slow modulation case by regarding our model as a stochastic two-state jump model and consider the mixture of the coherent and incoherent processes. Section 6 is devoted to the summary and conclusions.

§2. Time Evolution of Two-Level System

Let us consider an atomic two-level system described by a ground state $|0\rangle$ and a single excited state $|1\rangle$ with energy separation ω_0. For this system, annihilation and creation operators are denoted by a and a^+, respectively. The equation of motion for the density operator of this system interacting with a monochromatic laser is described by the quantal Liouville equation (*master equation*)[5,6]

$$\dot{\rho}(t)=-\mathrm{i}L(t)\rho(t), \tag{2.1}$$

where the quantal Liouvillian $L(t)$ is

$$-\mathrm{i}L(t)\rho\equiv-\mathrm{i}\omega_0(a^+a)^\times\rho+\mathrm{i}R(\mathrm{e}^{-\mathrm{i}\nu t}a^++\mathrm{e}^{\mathrm{i}\nu t}a)^\times\rho+\kappa a\rho a^+-\frac{1}{2}\kappa(a^+a)^\circ\rho, \tag{2.2}$$

in which κ is the natural radiation damping and ν is the frequency of the incident laser light. The constant R is the amplitude of the incident light expressed as the Rabi frequency. Assuming that $\nu\sim\omega_0$, the rotating-wave approximation is adapted for the coupling of the system with the laser light. The hyper-operators denoted by the superscripts, $\times$ and $\circ$, are defined by

$$\begin{aligned}F^\circ G&\equiv FG+GF,\\ F^\times G&\equiv FG-GF,\end{aligned} \tag{2.3}$$

for any operators F and G. The density operator $\rho(t)$ may be expanded in the form

$$\rho(t)=P_1(t)|1\,1\rangle\!\rangle+P_2(t)|0\,0\rangle\!\rangle+P_3(t)\,\mathrm{e}^{-\mathrm{i}\nu t}|1\,0\rangle\!\rangle+P_4(t)\,\mathrm{e}^{\mathrm{i}\nu t}|0\,1\rangle\!\rangle, \tag{2.4}$$

where we have introduced the notation

$$|i\rangle\langle j|=|ij\rangle\!\rangle. \tag{2.5}$$

The Liouvillian eq. (2.2) is expressed in terms of the expansion coefficients of eq. (2.4) as

$$\dot{\boldsymbol{P}}(t)=-\mathrm{i}\boldsymbol{L}\boldsymbol{P}(t). \tag{2.6}$$

Here, $\boldsymbol{P}(t)$ is the column vector with the components $P_j(t)$ $(j=1,\cdots,4)$ and $\mathrm{i}\boldsymbol{L}$ is the matrix

$$\mathrm{i}\boldsymbol{L}=\begin{bmatrix}\kappa & 0 & \mathrm{i}R & -\mathrm{i}R\\ -\kappa & 0 & -\mathrm{i}R & \mathrm{i}R\\ \mathrm{i}R & -\mathrm{i}R & \frac{1}{2}\kappa-\mathrm{i}\omega_1 & 0\\ -\mathrm{i}R & \mathrm{i}R & 0 & \frac{1}{2}\kappa+\mathrm{i}\omega_1\end{bmatrix}, \tag{2.7}$$

where we put $\omega_1=\nu-\omega_0$. Equation (2.6) with (2.7) is the well-known optical Bloch equation and parameters κ and $\frac{1}{2}\kappa$ correspond to the longitudinal and transverse relaxation rates, respectively. The Laplace transform of this is then

$$\boldsymbol{P}[s]=\frac{1}{\boldsymbol{S}+\mathrm{i}\boldsymbol{L}}\boldsymbol{P}(0), \tag{2.8}$$

where $\boldsymbol{S}$ is the unity matrix multiplied by the Laplace parameter s and the fractional expression means the inverse operator.

We now consider that the two-level atom is brought into contact with a heat bath as was treated in refs. 17 and 18. Namely, we assume the bath-system interaction linear in the coordinates of the bath oscillators which are eliminated with the use of Feynman-Vernon's influence functionals to yield the hyperoperator expression,

$$\rho[s]=\cfrac{1}{s+\mathrm{i}L+V^{\times}\cfrac{\Delta^2}{s+\gamma+\mathrm{i}L+V^{\times}\cfrac{2\Delta^2}{s+2\gamma+\mathrm{i}L+V^{\times}\cfrac{3\Delta^2}{s+3\gamma+\mathrm{i}L+\cdots}\Theta}\Theta}\Theta}\rho(0), \tag{2.9}$$

where

$$\Theta\equiv V^{\times}-\mathrm{i}\delta V^{\circ} \tag{2.10}$$

with

$$\delta=\beta\hbar\gamma/2. \tag{2.11}$$

Here, V is the operator of the test system coupled to the bath oscillators and Δ is the coupling constant. The constant γ and $\beta=1/k_BT$ are, respectively, the Debye relaxation rate and the initial temperature of the bath. The constants Δ and γ correspond to the modulation amplitude and rate in the stochastic theory respectively.

When the condition

$$\Delta\ll\gamma,\ \nu_{\mathrm{A}}, \tag{2.12}$$

is satisfied, the deeper stages of the continued fraction can be neglected. Here, ν_{A} is the characteristic frequency of the system. We write the matrix expression of $V^{\times}$ and Θ as $\boldsymbol{V}$ and $\boldsymbol{W}$. Then we can express the resolvent as

$$\boldsymbol{Z}[s]=\frac{1}{\boldsymbol{S}+\mathrm{i}\boldsymbol{L}+\boldsymbol{\Phi}(s)}, \tag{2.13}$$

where

$$\boldsymbol{\Phi}(s)=\boldsymbol{V}\frac{1}{\boldsymbol{S}+\boldsymbol{G}+\mathrm{i}\boldsymbol{L}}\boldsymbol{W}, \tag{2.14}$$

and $\boldsymbol{G}$ represents the diagonal matrix with the constant γ. Note that the condition eq. (2.12) secures the Gaussian property of the modulation, but we need not assume γ so large compared with Δ, since the continued fraction eq. (2.9) converges quickly even for not so large γ. We also note that, by neglecting the term of $\mathrm{i}\delta$, eq. (2.13) with (2.14) coincides with the resolvent of the stochastic two-state jump modulation model (see appendix of ref. 14), because in this approximation we take into account only two bath states defined by the path integrals, namely the equilibrium state and one-phonon excitation state of the bath. Thus, if we regard our bath as a two-state jump stochastic model, the condition, eq. (2.12), may be removed.

The inverse matrix eq. (2.13) can be analytically evaluated. The common denominator of the elements of the matrix eq. (2.13) is expressed in a polynomial of s as

$$(s-s_0)(s-s_1)(s-s_2)(s-s_3)\cdots(s-s_n). \tag{2.15}$$

One of the roots is $s_0=0$. Other roots s_1, $s_2,\cdots,s_n$ are evaluated numerically. Then, using the inverse Laplace transform of $\boldsymbol{Z}[s]$, we can express the time evolution of $\boldsymbol{P}(t)$ with the initial condition $\boldsymbol{P}(0)$ as

$$\boldsymbol{P}(t)=\boldsymbol{Z}(t)\boldsymbol{P}(0), \tag{2.16}$$

where

$$\boldsymbol{Z}(t)=\sum_{j=0}^{n}\boldsymbol{Z}_j\,\mathrm{e}^{s_jt}, \tag{2.17}$$

and

$$\boldsymbol{Z}_j\equiv(s-s_j)\boldsymbol{Z}[s]\,|_{s=s_j}. \tag{2.18}$$

Now we consider a squared pulse laser defined by

$$R\rightarrow\begin{cases}R & (0<t\leqq T)\\ 0. & (t>T)\end{cases} \tag{2.19}$$

The corresponding Liouvillian is then given by

$$L(t)\rightarrow\begin{cases}L & (0<t\leqq T)\\ L_0=L\,|_{R=0}. & (t>T)\end{cases} \tag{2.20}$$

The time evolution of $\boldsymbol{P}(t)$ is now described by

$$P(t)=\begin{cases} Z(t)P(0) & (0<t\leqq T) \\ C(t-T)Z(T)P(0)+U'(t-T)Q(T)P(0), & (t>T) \end{cases} \tag{2.21}$$

since the higher order interactions which were discussed in refs. 18 and 19 play an important role at the switching off time, T. Here, $C(t)$, $U'(t)$ and $Q(t)$ represent the inverse Laplace transform of the matrices,

$$C[s]=\frac{1}{S+\mathrm{i}L_0+\Phi_0(s)}, \tag{2.22}$$

$$U'[s]=C[s]V\frac{-\mathrm{i}\Delta}{S+G+\mathrm{i}L_0}, \tag{2.23}$$

and

$$Q[s]=\frac{-\mathrm{i}}{S+G+\mathrm{i}L}WZ[s], \tag{2.24}$$

where $\Phi_0(s)$ is obtained from eq. (2.14) by putting $R=0$.

For later convenience, we also define the following matrices:

$$Q'[s]=Z[s]V\frac{-\mathrm{i}\Delta}{S+G+\mathrm{i}L}, \tag{2.25}$$

$$Z'[s]=\frac{1}{S+G+\mathrm{i}L}+\frac{-\mathrm{i}\Delta}{S+G+\mathrm{i}L}WZ[s]\times V\frac{-\mathrm{i}\Delta}{S+G+\mathrm{i}L}$$

$$=\frac{1}{S+\mathrm{i}L+W\dfrac{\Delta^2}{S+G+\mathrm{i}L}V}, \tag{2.26}$$

$$C'[s]=\frac{1}{S+\mathrm{i}L_0+W\dfrac{\Delta^2}{S+G+\mathrm{i}L_0}V}, \tag{2.27}$$

and

$$U[s]=\frac{-\mathrm{i}\Delta}{S+G+\mathrm{i}L_0}WC[s]. \tag{2.28}$$

The denominator of eqs. (2.24–2.26) can be expressed as

$$(s+\gamma)(s-s_1)(s-s_2)(s-s_3)\cdots(s-s_n), \tag{2.29}$$

where the roots $s_1, s_2, \cdots, s_n$ are the same as those appearing in eq. (2.15). The denominators of eqs. (2.22), (2.23), (2.27) and (2.28) are analytically evaluated, but are not shown here.

§3. Physical Spectrum

Now we proceed to the formulation of density elements to the time-dependent physical spectrum. As was shown in ref. 16, the physical spectrum presented by Eberly and Wódkiewicz[1] can be written as

$$I(\omega, t)=4\Gamma_{\mathrm{f}}\exp[-2\Gamma_{\mathrm{f}}t]\,\mathrm{Re}\left\{\int_0^t \mathrm{d}t'\int_{t'}^t \mathrm{d}t''\exp[(\Gamma_{\mathrm{f}}+\mathrm{i}\omega)t']\exp[(\Gamma_{\mathrm{f}}-\mathrm{i}\omega)t'']C(t'', t')\right\}. \tag{3.1}$$

In this equation, Γ_{f} is the spectral bandwidth of the Fabry-Perot interferometer, and

$$C(t'', t')=\langle a^+(t'')a(t')\rangle=\mathrm{tr}\,\{\rho_{\mathrm{tot}}(0)a^+(t'')a(t')\} \tag{3.2}$$

is the correlation function of the dipole moment expressed by Heisenberg operators of atomic system $a^+(t)$, $a(t)$ and the density operator of the total system $\rho_{\mathrm{tot}}(0)$. Here, for simplicity, we have omitted the proportionality constant between the amplitude of the observed scattered light and the dipole moment. This equation includes the *coherent* and *incoherent* components. Following the CW study of Knight and Milonni,[7] we define the coherent component of the correlation function by

$$C_{\mathrm{coh}}(t'', t')=\langle a^+(t'')\rangle\langle a(t')\rangle=\mathrm{tr}\,\{\rho_{\mathrm{tot}}(0)a^+(t'')\}\,\mathrm{tr}\,\{\rho_{\mathrm{tot}}(0)a(t')\}. \tag{3.3}$$

We write the coherent spectrum calculated from this term as $I_{\mathrm{coh}}(\omega, t)$. By subtracting eq. (3.3) from eq. (3.2), the incoherent element may be expressed as

$$C_{\mathrm{inc}}(t'', t')=C(t'', t')-C_{\mathrm{coh}}(t'', t')=\langle(a^+(t'')-\langle a^+(t'')\rangle)(a(t')-\langle a(t')\rangle)\rangle. \tag{3.4}$$

The incoherent spectrum denoted by $I_{\rm inc}(\omega, t)$ can be evaluated from the above equation in principle, but practical calculations will be done by subtracting $I_{\rm coh}(\omega, t)$ from eq. (3.1).

For the total Liouvillian $L(t)$ and the density operator $\rho(t)$, $C(t'', t')$ can be expressed in the operator form as[13]

$$C(t'', t')=\mathrm{tr}\left\{a^{+}\overleftarrow{\exp}\left[-\mathrm{i}\int_{t'}^{t''}L(\tau)\,\mathrm{d}\tau\right](a\rho(t'))\right\}, \tag{3.5}$$

where the arrow indicates the ordered exponential. This function can be evaluated by using the matrix expression of $\mathrm{i}L(t)$ and $\rho(t)$.

3.1 CW response

First we present the physical spectrum of the CW response in order to make references of the time-dependent spectrum. For the CW excitation Liouvillian eq. (2.7), we may write the physical spectrum of eq. (3.1) as

$$I(\omega, t)=4\Gamma_{\rm f}\exp\left[-2\Gamma_{\rm f}t\right]\mathrm{Re}\left\{\int_0^t \mathrm{d}t'\int_{t'}^{t}\mathrm{d}t''g(t')g^{*}(t'')C_1(t'', t')\right\}. \tag{3.6}$$

Here, $g(t)=\exp\left[\{\Gamma_f+\mathrm{i}(\omega_2-\omega_1)\}t\right]$ with $\omega_2=\omega-\omega_0$ and the correlation function is defined by

$$C_1(t'', t')=\boldsymbol{T}\boldsymbol{D}^{+}\boldsymbol{Z}(t''-t')\boldsymbol{D}^{-}\boldsymbol{P}(t')+\boldsymbol{T}\boldsymbol{D}^{+}\boldsymbol{Q}'(t''-t')\boldsymbol{D}^{-}\boldsymbol{P}'(t'), \tag{3.7}$$

in which

$$\boldsymbol{P}(t')=\boldsymbol{Z}(t')\boldsymbol{P}(0),\quad \boldsymbol{P}'(t')=\boldsymbol{Q}(t')\boldsymbol{P}(0). \tag{3.8}$$

The matrices $\boldsymbol{T}$, $\boldsymbol{D}^{+}$ and $\boldsymbol{D}^{-}$ are, respectively, defined as

$$\boldsymbol{T}=[1\ 1\ 0\ 0], \tag{3.9}$$

$$\boldsymbol{D}^{-}=\begin{bmatrix}0&0&0&0\\0&0&1&0\\0&0&0&0\\1&0&0&0\end{bmatrix},\quad \boldsymbol{D}^{+}=\begin{bmatrix}0&0&0&1\\0&0&0&0\\0&1&0&0\\0&0&0&0\end{bmatrix}. \tag{3.10}$$

By taking the limit $t\to\infty$, the CW spectrum is obtained from eq. (3.6) with eq. (3.7). Changing parameters as $\tau=t''-t'$ and $\tau'=t-(t'+t'')/2$ and performing the integrations in eq. (3.6), we have

$$I(\omega)=2\,\mathrm{Re}\left\{\boldsymbol{T}\boldsymbol{D}^{+}\boldsymbol{Z}[s]\boldsymbol{D}^{-}\boldsymbol{P}^{\rm e}+\boldsymbol{T}\boldsymbol{D}^{+}\boldsymbol{Q}'[s]\boldsymbol{D}^{-}\boldsymbol{P}'^{\rm e}\right\}|_{s=\Gamma_{\rm f}+\mathrm{i}(\omega_2-\omega_1)}, \tag{3.11}$$

where the equilibrium density vectors $\boldsymbol{P}^{\rm e}$ and $\boldsymbol{P}'^{\rm e}$ are defined by

$$\boldsymbol{P}^{\rm e}=\lim_{s_0\to 0}s_0\boldsymbol{Z}[s_0]\boldsymbol{P}(0),\quad \boldsymbol{P}^{\rm e'}=\lim_{s_0\to 0}s_0\boldsymbol{Q}[s_0]\boldsymbol{P}(0). \tag{3.12}$$

The initial conditions are assumed to be $P_2(0)=1$ and $P_1(0)=P_3(0)=P_4(0)=0$. Then eq. (3.11) is expressed in the matrix elements as

$$I(\omega_2)=2\,\mathrm{Re}\left\{Z_{42}[s]P_3^{\rm e}+Z_{44}[s]P_1^{\rm e}+Q'_{42}[s]P_3'^{\rm e}+Q'_{44}[s]P_1'^{\rm e}\right\}|_{s=\Gamma_{\rm f}+\mathrm{i}(\omega_2-\omega_1)}. \tag{3.13}$$

3.2 Pulse response

Now we present the time-dependent physical spectrum driven by the pulsed laser eq. (2.19). For the time $t<T$, the physical spectrum $I(\omega, t)$ is calculated from eq. (3.6). For the time $T+\tau$, this is given by

$$I(\omega, T+\tau)=4\Gamma_1 \exp[-\Gamma_1(T+\tau)]\,\mathrm{Re}\left(\int_0^T dt'\int_{t'}^T dt''g(t')g^*(t'')C_1(t'',t')\right.$$
$$+\int_0^T dt'\int_{t'}^{T+\tau} dt''g(t')g^*(t'')C_2(t'',t')$$
$$\left.+\int_0^{T+\tau} dt'\int_{t'}^{T+\tau} dt''g(t')g^*(t'')C_3(t'',t')\right). \tag{3.14}$$

Here,

$$C_2(t'',t')=\boldsymbol{T}\boldsymbol{D}^+\boldsymbol{C}(t''-T)\{\boldsymbol{Z}(T-t')\boldsymbol{D}^-\boldsymbol{P}(t')+\boldsymbol{Q}'(T-t')\boldsymbol{D}^-\boldsymbol{P}'(t')\}$$
$$+\boldsymbol{T}\boldsymbol{D}^+\boldsymbol{U}'(t''-T)\{\boldsymbol{Q}(T-t')\boldsymbol{D}^-\boldsymbol{P}(t')+\boldsymbol{Z}'(T-t')\boldsymbol{D}^-\boldsymbol{P}'(t')\}, \tag{3.15}$$

and

$$C_3(t'',t')=\boldsymbol{T}\boldsymbol{D}^+\boldsymbol{C}(t''-t')\{\boldsymbol{C}(t'-T)\boldsymbol{D}^-\boldsymbol{P}(T)+\boldsymbol{U}'(t'-T)\boldsymbol{D}^-\boldsymbol{P}'(T)\}$$
$$+\boldsymbol{T}\boldsymbol{D}^+\boldsymbol{U}'(t''-t')\{\boldsymbol{U}(t'-T)\boldsymbol{D}^-\boldsymbol{P}(T)+\boldsymbol{C}'(t'-T)\boldsymbol{D}^-\boldsymbol{P}'(T)\}. \tag{3.16}$$

We consider the case that, before the pulse excitation, the test system reaches the equilibrium state $\boldsymbol{P}_0^e$ under the bath modulation, which is evaluated from eq. (3.12) by putting $R=0$. Since the bath-system interaction does not excite the system for a diagonal modulation model, which will be discussed in §4, $\boldsymbol{P}_0^e$ coincides with the initial state $\boldsymbol{P}(0)$. Then the matrices $\boldsymbol{P}(t)$ and $\boldsymbol{P}'(T)$ of the above equations may be evaluated from eq. (3.8). The coherent component is evaluated by

$$C_{\mathrm{coh}}(t'',t')=P_4(t')P_3(t''). \tag{3.17}$$

Here, $P_j(t)$ is calculated from eq. (2.21).

§4. Diagonal Modulation Model

If we suppose that the bath interactions with the system are diagonal, then

$$V=a^+a. \tag{4.1}$$

This interaction induces the fluctuation of the atomic resonance frequency and has been studied extensively in the stochastic approach.[11-15] The CW response spectrum of a similar system was studied by Tsunetsugu and Hanamura from the stochastic Gaussian-Markoffian approach.[15] For the interaction eq. (4.1), hyperoperators $V^\times$ and Θ are, respectively, given in the matrix form as

$$\boldsymbol{V}=\begin{bmatrix}0&0&0&0\\0&0&0&0\\0&0&1&0\\0&0&0&-1\end{bmatrix},\quad \boldsymbol{W}=\begin{bmatrix}0&0&0&0\\0&0&0&0\\0&0&1-i\delta&0\\0&0&0&-1-i\delta\end{bmatrix}. \tag{4.2}$$

Then the effect of modulation eq. (2.14) is evaluated as

$$\boldsymbol{\Phi}(s)=\begin{bmatrix}0&0&0&0\\0&0&0&0\\0&0&\Gamma(s)&\Gamma'^*(s)\\0&0&\Gamma'(s)&\Gamma^*(s)\end{bmatrix}, \tag{4.3}$$

where

$$\Gamma(s)=\frac{(1-i\delta)\Delta^2\left\{\left(s+\gamma+\frac{1}{2}\kappa+i\omega_1\right)(s+\gamma+\kappa)+2R^2\right\}}{2R^2(2s+2\gamma+\kappa)+(s+\gamma+\kappa)\left[\left(s+\gamma+\frac{1}{2}\kappa\right)^2+\omega_1^2\right]}, \tag{4.4}$$

$$\Gamma'(s)=\frac{-2(1-i\delta)\Delta^2R^2}{2R^2(2s+2\gamma+\kappa)+(s+\gamma+\kappa)\left[\left(s+\gamma+\frac{1}{2}\kappa\right)^2+\omega_1^2\right]}. \tag{4.5}$$

The time evolution of the two-level system is determined by eq. (2.13). Functions $\Gamma(s)$ and $\Gamma'(s)$ act on this equation as the damping and the shift. When γ and Δ satisfy the condition (*motional narrowing limit*)

$$\Delta/\gamma\ll 1 \quad \text{with} \quad \Delta^2/\gamma=\gamma', \tag{4.6}$$

the off-diagonal term, $\Gamma'(s)$, tends to zero, whereas the diagonal term, $\Gamma(s)$, tends to $\gamma'-i\beta\hbar\gamma'/2$. Thereby, in eq. (2.13), the effect of modulation in the narrowing limit can be regarded as the additional transverse damping and the shift of the atomic resonance frequency.

4.1 CW response

The CW response spectrum is calculated from eq. (3.13). First we discuss the coherent component $I_{\rm coh}(\omega_2)$. Here, we set $\Gamma_f=0$ to compare with the previous stochastic results.[14] The elements of $\boldsymbol{Z}[s]$ have the pole at $s=0$, whereas elements of $\boldsymbol{Q}'[s]$ have the pole at $s=-\gamma$. The pole $s=0$ gives rise to the delta-shaped peak at the incident laser frequency $\omega_1=\omega_2$ which is called the pure Rayleigh component and agrees with the coherent component calculated from eq. (3.3) as

$$\begin{aligned}I_{\rm coh}(\omega_2)&=2\pi\delta(\omega_2-\omega_1)P_3^e\cdot P_4^e\\&=2\pi\delta(\omega_2-\omega_1)\\&\quad\times\frac{\kappa^2R^2\left|\frac{1}{2}\kappa-i(\omega_2-\omega_1)+\Gamma(0)+\Gamma'(0)\right|^2}{\left\{\kappa\left[\left|\frac{1}{2}\kappa-i(\omega_2-\omega_1)+\Gamma(0)\right|^2-\Gamma'(0)^2\right]+4R^2\,\mathrm{Re}\left[\frac{1}{2}\kappa+\Gamma(0)+\Gamma'(0)\right]\right\}^2}.\end{aligned} \tag{4.7}$$

For a weak incident light, namely where κ, γ, $(\omega_2-\omega_1)\gg R$, this equation becomes

$$I_{\rm coh}(\omega_2)=2\pi\delta(\omega_2-\omega_1)\frac{R^2}{\left|\frac{1}{2}\kappa+\Lambda(\omega_1)+i\omega_1\right|^2}, \tag{4.8}$$

where

$$\Lambda(\omega_1)=\frac{\Delta^2}{\gamma+i\omega_1}. \tag{4.9}$$

This result agrees with those of the second-order optical process of the stochastic two-state jump modulation model,[11,14] since in this case of weak incident light, the higher order optical processes can be neglected.

Next we discuss the incoherent component $I_{\rm inc}(\omega_2)$. This component can be evaluated in an analytical form. However, despite the simplicity, the resulting expressions are quite lengthy therefore here we only present the numerical results. Note that the pole $s=-\gamma$ of this component yields a Lorentzian peak with the width γ at $\omega_2=\omega_1$ overlapping the pure-Rayleigh peak. This component bears a mixed character of the coherent and incoherent processes and is called the broadened Rayleigh component.[11-15] The width of this peak is $1/\gamma$ and is negligible in this fast modulation region. This element is discussed in §5, by regarding our model as the stochastic two-state jump model.

Figure 1 shows the CW spectra of the fluorescence light for different field strength. The other parameters are chosen as:

$$\kappa=1, \quad \omega_1=30, \quad \Delta=10,$$
$$\gamma=50, \quad \delta=0, \quad \Gamma_f=0.001. \quad (4.10)$$

The δ-shaped coherent component is not shown in the figures. Since $i\delta$ is small compared with other parameters, the reaction effects of the bath do not play a role in this example. In Fig. 1(a) the fluorescence (luminescence) peak corresponding to the second-order optical process appears at the atomic resonance position ($\omega_2=0$). Since Δ is so small compared with γ, the broadened Rayleigh component at the incident frequency $\omega_2=30$ is unnoticeable. Figure 1(b) shows the emission spectrum for a stronger laser excitation. In this case, higher order optical processes become dominant and a fluorescence peak also appears at $\omega_2=30$, while the peak at the atomic resonance frequency $\omega_2=0$ is slightly shifted by the mechanism of the dynamical (AC) Stark effect.[6,7] In Fig. 1(c) of the very strong excitation, three splitting peaks appear at the laser frequency $\omega_2=30$ and at the satellite positions corresponding to

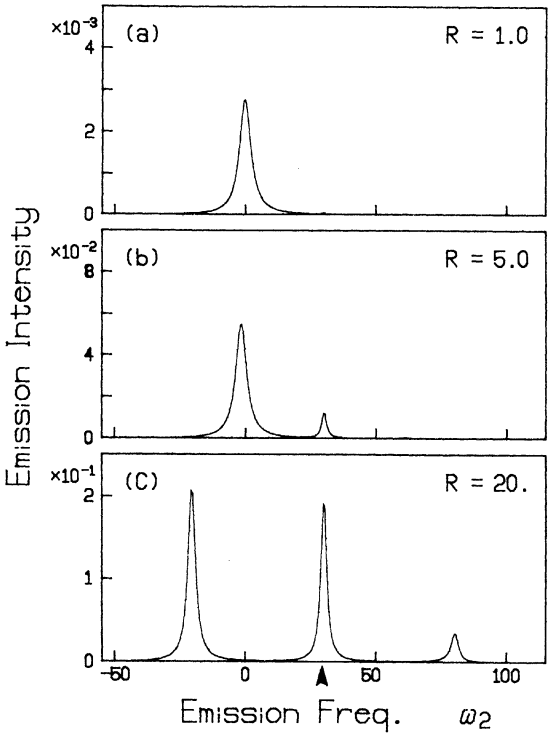

Fig. 1. Emission spectra for various strengths of excitation field R with the fast modulation. In this figure (and the following figures) an arrow indicates the position of the laser frequency ω_1. The δ-shaped Rayleigh peaks located at $\omega_2=30$ are not shown in the figures but their heights are given by (a) 7.2×10^{-3}, (b) 1.2×10^{-1} and (c) 2.0×10^{-1}.

the virtual Stark levels at about $\omega_2=-20$ and 80. As was discussed in ref. 6, if the natural radiation damping was the only mechanism of the relaxation process, these Stark satellites should show the same height at symmetrical positions. But when the bath modulation is imposed, the peak arising from the virtual level closer to the atomic resonance level $\omega_2=0$ becomes higher than the other, since the resonance absorption caused by the fluctuation of the resonance frequency gives rise to the additional fluorescence processes which decay from the virtual level near the atomic resonance frequency.[7-10]

4.2 *Pulse response*

The time-dependent spectrum driven by the pulsed laser is calculated from eq. (3.14). The numerical examples are shown in Figs. 2-4. In these figures, the parameters are chosen as the following:

$$\kappa=1, \quad \omega_1=30, \quad \Delta=10, \quad \gamma=50,$$
$$\delta=0.01, \quad T=2, \quad \Gamma_f=1. \quad (4.11)$$

Figures 2(a) and 2(b) illustrate the incoherent and coherent components driven by the weak incident pulse which corresponds to the second-order optical process. At the very first stage, both coherent and incoherent spectrum are broadened, since there is a frequency uncertainty of the order t^{-1}. Then the peaks increase as time proceeds. In Fig. 2(a) of the incoherent component, the peak appears at the atomic resonance position $\omega_2=0$. This peak increases about $t=2.5$ even though the pulse is switched off, since spontaneous emission occurs at the atomic resonance position after the pulse with the mechanism of the relaxation processes. In Fig. 2(b) of the coherent component, the peak appears at the incident laser frequency $\omega_2=30$. The build-up speed of this peak is faster than the incoherent one. Small peaks appear temporarily at the resonance position beginning when the pulse is switched on ($t=0$) as well as when it is switched off ($t=T$). The existence of these peaks suggests that we cannot distinguish the coherent component only from its position in the time-dependent spectrum. After the pulse, the main peak of the coherent component quickly decreases with the filter bandwidth Γ_f and the transverse

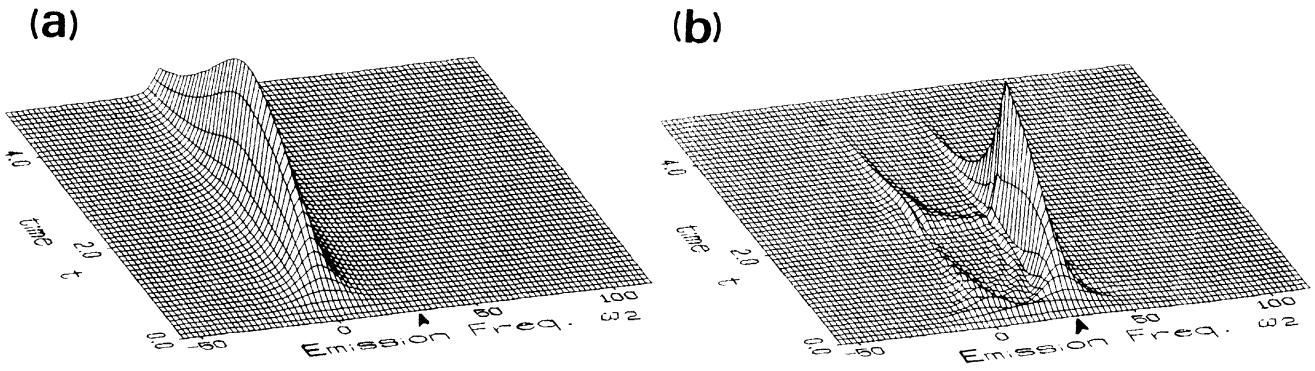

Fig. 2. Time-dependent emission spectrum from a two-level atom (a) the incoherent component and (b) the coherent component for a weak pulse strength $R=1$ with $\gamma=50$. The pulse is switched off at $t=2.0$. For reference, the maximum value of (a) at $t=2.5$ and $\omega_2=0.0$ is 1.6×10^{-3} and that of (b) at $t=2.0$ and $\omega_2=30$ is 1.7×10^{-3}.

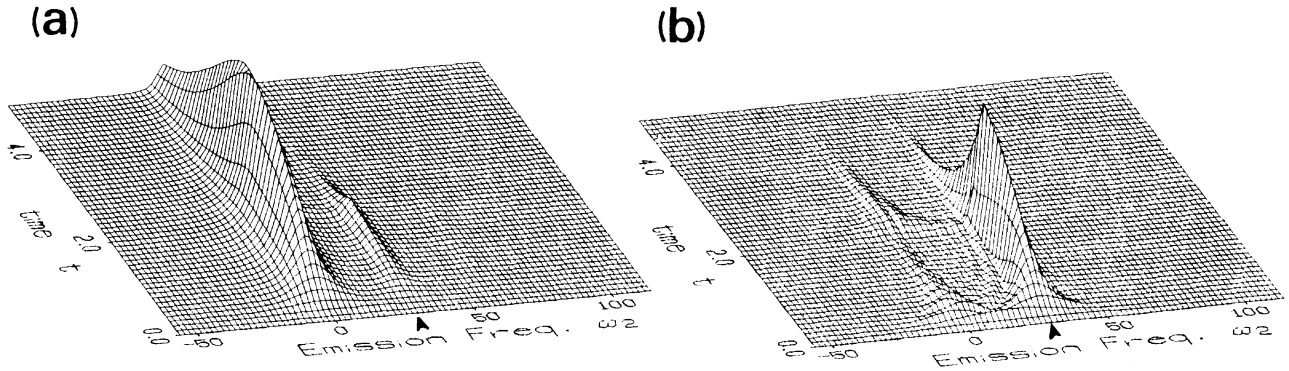

Fig. 3. Same as Fig. 2 except a pulse strength $R=5$. For reference, the maximum value of (a) at $t=2.3$ and $\omega_2=-2.0$ is 3.2×10^{-2} and that of (b) at $t=2.0$ and $\omega_2=30$ is 3.1×10^{-2}.

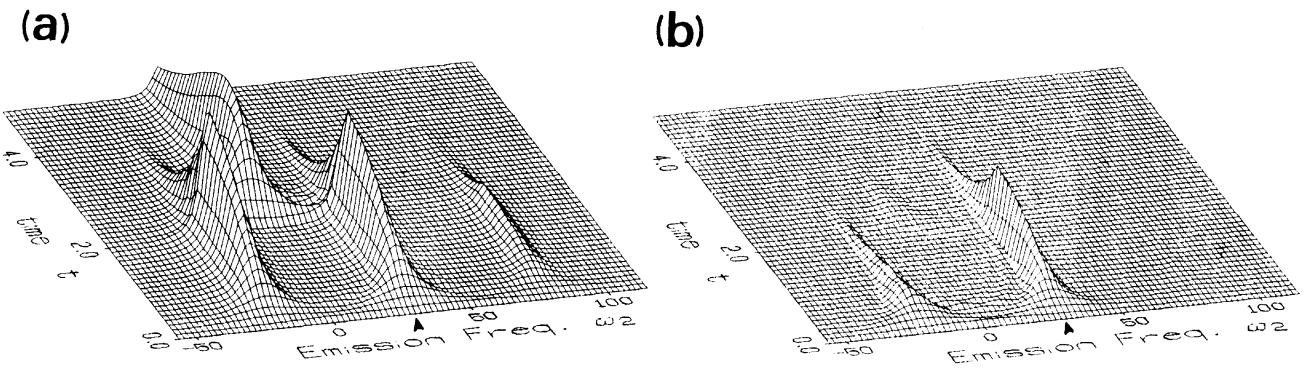

Fig. 4. Same as Fig. 2 except a strong pulse strength $R=20$. For reference, the maximum value of (a) at $t=2.0$ and $\omega_2=-20$ is 1.1×10^{-1} and that of (b) at $t=2.0$ and $\omega_2=30$ is 5.6×10^{-2}.

relaxation rate of eq. (2.21). Figures 3(a) and 3(b) show results for a strong pulse, $R=5$. In Fig. 3(a) of the incoherent component, the peak at the laser frequency is the fluorescence of higher order optical processes and, after the pulse, this quickly disappears. In Fig. 3(b), qualitative features of the coherent component do not change from the weak incident case of Fig. 2(b). Figures 4(a) and 4(b) show results for a very strong incident pulse. In Fig. 4(a), during the pulse excitation, three Stark peaks appear at the incident laser frequency and virtual Stark levels. When the pulse is switched off, these Stark peaks decrease quickly, since the virtual levels vanish with the pulse. The spontaneous emission peak builds

up at the atomic resonance position. In Fig. 4(b) the coherent component becomes small compared to the incoherent process. However, qualitative features are not changed.

§5. Two-State Jump Modulation

In the previous section, we regard our model as an approximation of the dynamical system interacting with a stochastic Gaussian-Markoffian bath. But our model can also apply to the slow or strong modulation case by regarding the model as the stochastic two-state jump modulation with the amplitude Δ and modulation rate γ.[11,14] In the following discussion, parameters are the same as eqs. (4.10) and (4.11) except $\gamma=3$.

The CW response spectra are given in Fig. 5. The δ-shaped coherent component is not shown in figure. In the weak incident case of Fig. 5(a), two luminescence peaks appear at the two possible stochastic levels, $-\Delta$ and Δ ($\Delta=10$). The peak at $\omega_2=30$ is the broadened Rayleigh component, as discussed in refs. 11 and 14. In Fig. 5(b), the central peak of the dynamical Stark component appears at the incident laser frequency $\omega_2=30$ overlapping the broadened Rayleigh peak and they can not be distinguished. In Fig. 5(c) of the very strong field, two possible levels, $\pm\Delta$, show the dynamical Stark splitting, and five peaks appear.

The time-dependent spectra are given in Figs. 6-8. The coherent components are not shown here, since the qualitative features of these are similar to the fast modulation case. Figure 6 shows results for weak excitation. In this figure, peaks at $\omega_2=-\Delta$ and Δ ($\Delta=10$) are fluorescence peaks and $\omega_2=30$ is the broadened Rayleigh component. The broadened Rayleigh peak is wider than the coherent component. The time evolution of the broadened Rayleigh is similar to that of the coherent peak, but it decays faster than the coherent one after the pulse excitation is terminated. For the strong excitation case of Fig. 7, the fluorescence of the higher order optical process appears at the incident laser frequency during the pulse excitation, and can not be distinguished from the broadened Rayleigh component. For a very strong excitation of

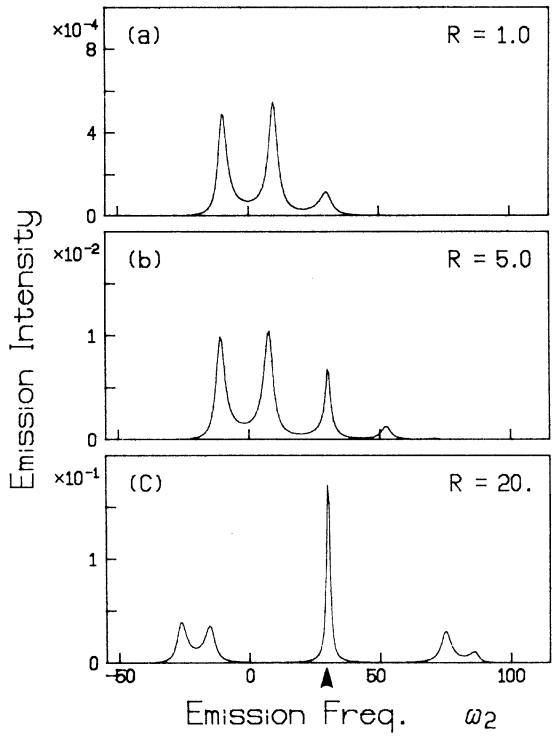

Fig. 5. Emission spectra of a two-state jump modulation model for various strengths of excitation field R with slow modulation $\gamma=3$. The delta-shaped Rayleigh peaks located at $\omega_2=30$ not shown in the figures are given by (a) 8.7×10^{-3}, (b) 1.7×10^{-1} and (c) 5.7×10^{-1}.

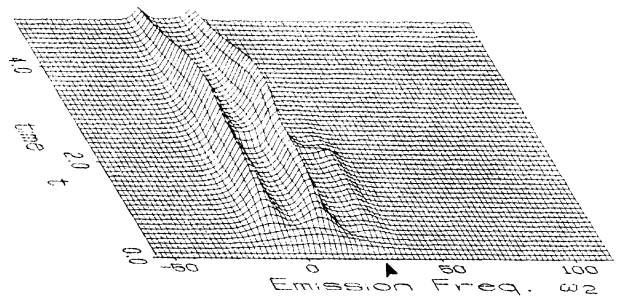

Fig. 6. Time-dependent spectrum of the incoherent component of the two-state jump modulation model for a weak pulse strength $R=1$. The modulation ratio is chosen as $\gamma=3$. For reference, the maximum value of the figure at $t=2.8$ and $\omega_2=10$ is 5.0×10^{-4}.

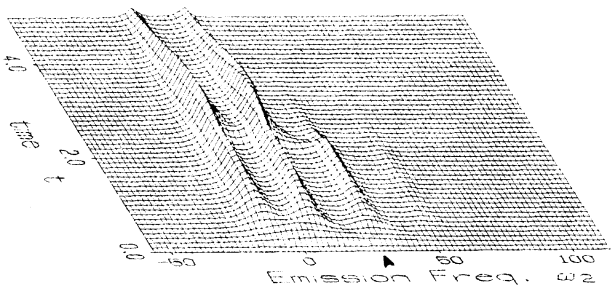

Fig. 7. Same as Fig. 6 except a pulse strength $R=5$. For reference, the maximum value of the figure at $t=2.6$ and $\omega_2=8.0$ is 9.9×10^{-3}.

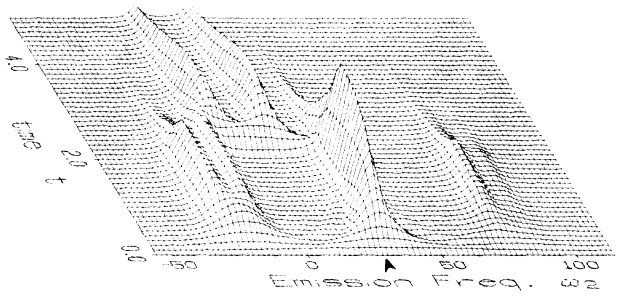

Fig. 8. Same as Fig. 6 except a strong pulse strength $R=20$. For reference, the maximum value of the figure at $t=2.5$ and $\omega_2=30$ is 8.9×10^{-2}.

Fig. 8, five Stark splitting peaks appear and, after the pulse, these peaks quickly decrease and spontaneous emission peaks build up at two possible stochastic levels. The build-up speed is slower than that of the corresponding peaks of Fig. 4, since the relaxation caused by the random perturbation is slower.

§6. Summary and Conclusions

In this paper we formulated the physical spectrum of a two-level atom driven by the CW and pulsed laser coupled to the finitely correlated bath. The emission spectrum was separated into the coherent and incoherent components and the time evolution of each component was discussed for various conditions.

Using these formulae, we investigated the CW and the pulse response spectrum for the diagonal modulation model. From the CW study, we show that, for weak excitation, the higher order optical processes can be neglected and the single fluorescence peak appears at the atomic resonance position corresponding to the second-order optical process. For strong excitation, the higher order optical processes play a role and three Stark peaks appear at the laser frequency and the corresponding two virtual-Stark levels. The side peak near the atomic resonance position becomes larger than the other peak. From the study of the pulse response, we see that the time evolution of the coherent component, except transient peaks appearing at the atomic resonance position, follows the pulse envelope, whereas the incoherent components do not follow, since the evolution of the incoherent component is governed not only by the pulse excitation but also by the relaxation processes. For a weak excitation pulse, the fluorescence peak corresponding to the second-order optical process appears and evolves in time. Since spontaneous emission occurs, this peak increases for a moment after the pulse. For strong excitation, the dynamical Stark splitting occurs during the pulse excitation. The Stark peaks decrease quickly when the pulse is switched off and the spontaneous emission peaks at the atomic resonance position build up. For all ranges of excitation, qualitative features of the coherent component do not change.

We confined ourselves to the relatively fast modulation region in §4. But we also examined the slow modulation region in §5 by regarding our model as stochastic two-state jump model. The characteristic feature of this case is that there appears a mixture of the coherent-incoherent process called the broadened Rayleigh at the laser frequency. Although the realistic system does not show the two-state jump characteristic, this treatment is useful to obtain insight into the nature of the coherent-incoherent mixed character. Extension of the analysis to the case of a general Gaussian-Markoffian bath is important and of great interest. We leave this extension for future study.

We conclude this work by pointing out that the responses to short pulsive excitations are generally fairly complicated and that they do not directly reveal the natures of the dynamical processes the atom may experience in the excited states. Clarification of this point is also left for future study.

References

1) J. H. Eberly and K. Wódkiewicz: J. Opt. Soc. Am. **67** (1977) 1252.
2) J. H. Eberly, C. V. Kunasz and K. Wódkiewicz: J. Phys. **B13** (1980) 217.
3) M. Aihara and A. Kotani: Solid State Commun. **59** (1983) 751.
4) T. Takagahara: Phys. Rev. A**35** (1987) 2493.
5) B. R. Mollow and M. M. Miller: Ann. Phys. **52** (1969) 464.
6) B. R. Mollow: Phys. Rev. **188** (1969) 1969.
7) P. L. Knight and P. W. Milonni: Phys. Rep. **66** (1980) 21.
8) B. R. Mollow: Phys. Rev. A**15** (1977) 1023.
9) J. L. Carlsten, A. Szöke and M. G. Raymer: Phys. Rev. A**15** (1977) 1029.
10) J. Cooper, R. J. Ballagh and K. Burnett: Phys. Rev. A**22** (1980) 535.

11) T. Takagahara, E. Hanamura and R. Kubo: J. Phys. Soc. Jpn. **43** (1977) 802.
12) T. Takagahara, E. Hanamura and R. Kubo: J. Phys. Soc. Jpn. **43** (1977) 811.
13) T. Chikama, K. Saikawa and R. Kubo: J. Phys. Soc. Jpn. **53** (1984) 991.
14) Y. Tanimura, H. Takano and R. Kubo: J. Phys. Soc. Jpn. **55** (1986) 4550.
15) H. Tsunetsugu and E. Hanamura: J. Phys. Soc. Jpn. **55** (1986) 3636.
16) J. Czub and S. Kryszewski: J. Phys. B**16** (1983) 3171.
17) Y. Tanimura and R. Kubo: J. Phys. Soc. Jpn. **58** (1989) 101.
18) Y. Tanimura and R. Kubo: J. Phys. Soc. Jpn. **58** (1989) 1199.
19) Y. Tanimura, T. Suzuki and R. Kubo: J. Phys. Soc. Jpn. **58** (1989) 1850.